DOI 10.1007/s11182-021-02471-7
Russian Physics Journal, Vol. 64, No. 8, December, 2021 (Russian Original No. 8, August, 2021)

DIURNAL DYNAMICS OF THE KINETIC ENERGY IN THE ATMOSPHERIC BOUNDARY LAYER RETRIEVED FROM MINISODAR MEASUREMENTS

A. I. Potekaev,[1] L. G. Shamanaeva,[1,2] and V. V. Kulagina[3] UDC 551.501.755; 551.501.796

Based on the results of postprocessing of minisodar measurements of three wind velocity components and their variances in the lower 200-meter layer of the atmosphere, the diurnal hourly dynamics of the kinetic energy of the atmosphere reduced to unit air mass and its component E_{TKE} (caused by turbulent pulsations of the wind velocity) and E_{MKE} (caused by the mean wind velocity) are analyzed focusing on the turbulent kinetic energy. It is shown that during 24 hour continuous minisodar observations, E_{TKE} was low up to 50 m, increased from 50 to 100 m, and fast increased at higher altitudes. A significant influence of the time of day on the observation results was noted. Thus, at night the kinetic energy did not exceed 20 J/kg and then increased with time from 20 to 50 J/kg. It reached a maximum in the morning. After sunrise, the turbulent kinetic energy quickly decreased, and the system underlying surface – near-surface air layer went into equilibrium. As a consequence, the spread of turbulent kinetic energy values decreased. The most significant changes were observed at altitudes of 100–200 m.Tthe time of day had no significant influence at altitudes of 50–100 m, and the E_{TKE} values were low and remained practically unchanged with time. Irrespective of the time of day, the maximum turbulent kinetic energy was observed at altitudes of 100–200 m, which poses the greatest danger to unmanned aerial vehicles. The corresponding numerical estimations are presented.

Keywords: atmospheric boundary layer, kinetic energy of the atmosphere per unit air mass, acoustic sounding, minisodar, turbulence, diurnal dynamics.

INTRODUCTION

The kinetic energy plays an important role in physics of the atmospheric boundary layer (ABL), study of its structure and dynamics, development of adequate physical representations, and construction of realistic mathematical models [1–3]. It is one of the ABL characteristics determining global and local circulations in the atmosphere and angular momentum, heat, and moisture transfer. Moreover, it is necessary to forecast and to calculate fields of meteorological parameters and diffusion of polluting impurities and to analyze and to predict conditions of acoustic radiation propagation. Recently, the urgency of research of ABL physics has considerably increased in connection with revolutionary development and application of unmanned aerial vehicles (UAV) [4] which, as a rule, are made of lightweight materials, used in the ABL (especially micro- and mini-dimensional UAV), and therefore, are strongly affected by the turbulent kinetic energy.

Nowadays a number of methods for measuring and predicting the average values and variances of the wind velocity components in the ABL have been developed using lidars, sodars, and radars (for example, see [5–8]). Each of them has its own advantages and disadvantages. For example, the refractive index of sound waves is by about 10^6 times

[1]National Research Tomsk State University, Tomsk, Russia, e-mail: potekaev@spti.tsu.ru; [2]V. E. Zuev Institute of Atmospheric Optics of the Siberian Branch of the Russian Academy of Sciences, Tomsk, Russia, e-mail: sima@iao.ru; [3]Siberian Medical University, Tomsk, Russia, e-mail: kulagina.vv@mail.ru. Translated from Izvestiya Vysshikh Uchebnykh Zavedenii, Fizika, No. 8, pp. 16–24, August, 2021. Original article submitted October 8, 2020.

higher than for radio and optical waves. Strong interaction of sound waves with the atmosphere together with the possibility of obtaining information round the clock in real time with much higher spatial and time resolution makes sodar the unique tool for investigation of the wind velocity field in the ABL.

The application of minisodars allows long time numbers of continuous observations of vertical profiles of both mean values and variances of three wind velocity components to be obtained simultaneously and their spatiotemporal dynamics to be analyzed [3, 7, 9]. Moreover, the data with high spatial (to several meters) and temporal resolutions (statistically reliable profiles of wind velocity components can be obtained with averaging, as a rule, from 1 to 30 min). Therefore, minisodar measurements are used to estimate the kinetic energy of both average and turbulent wind velocity components. Thus, in [9] preliminary results of analysis of the spatiotemporal dynamics of the turbulent kinetic energy of unit air mass from data of minisodar measurements were presented.

In this work, the diurnal hourly dynamics of the total kinetic energy of the atmosphere $E(z, t)$ and its components – the kinetic energy of ordered motion E_{MKE} (associated with the mean wind velocity) and the turbulent kinetic energy E_{TKE} (associated with the wind velocity variance) – obtained by postprocessing of minisodar measurements in the atmosphere at altitudes of 5–200 m are analyzed. The time periods and altitude ranges with high and low turbulence, that is, the most and least favorable for UAV flights are determined. These estimations are especially important for UAV made of lightweight polyfoams that have sufficiently large sizes (1–2 m).

APPLIED METHODS AND APPROACH

The total kinetic energy of the ABL $E_\Sigma = mV^2/2$ is defined by the energy of motion of air masses – the wind energy. Below we consider the kinetic energy reduced per unit mass $E = E_\Sigma / m$, in $\mathrm{m^2/s^2}$ ($1\ \mathrm{m^2/s^2} = 1$ J/kg). It is natural that the total kinetic energy of the atmosphere follows patterns established for the reduced kinetic energy. For this reason, below we use the term *kinetic energy* for the reduced kinetic energy. It is equal to the sum of two components: the mean kinetic energy E_{MKE}, associated with the mean wind velocity, and the turbulent kinetic energy E_{TKE}, associated with the wind velocity variance. The mean kinetic energy of unit air mass can be represented in the form [1–3]

$$\begin{aligned}\overline{E}(\boldsymbol{r},t) = \left(\overline{E}_{\mathrm{MKE}}(\boldsymbol{r},t) + \overline{E}_{\mathrm{TKE}}(\boldsymbol{r},t)\right)/m = \left(\left\langle V_x{}^2(\boldsymbol{r},t)\right\rangle + \left\langle V_y{}^2(\boldsymbol{r},t)\right\rangle + \left\langle V_z{}^2(\boldsymbol{r},t)\right\rangle\right)/2 \\ + \left(\left\langle \sigma_x^2(\boldsymbol{r},t)\right\rangle + \left\langle \sigma_y^2(\boldsymbol{r},t)\right\rangle + \left\langle \sigma_z^2(\boldsymbol{r},t)\right\rangle\right)/2,\end{aligned} \tag{1}$$

where $\boldsymbol{r} = (x, y, z)$, t is the observation time, the angular brackets denote averaging over a series of measurements, V_x V_y, and V_z are the wind velocity components, and σ_x^2, σ_y^2, and σ_z^2 are their variances. In this case, changes of terms enclosed in the parentheses will define $\overline{E}_{\mathrm{MKE}}$ and $\overline{E}_{\mathrm{TKE}}$ values, respectively. The diurnal hourly dynamics of the kinetic energy was calculated from formula (1) from minisodar measurements averaged over 10 minute periods with spatial resolutions $\Delta z = 5$ m. This allowed us to analyze the relative contributions of its components to the total kinetic energy.

Measurements were performed with the minisodar having working frequency of 4900 Hz, radiation pulse duration $\tau = 60$ ms, and pulse repetition period of 4 s. Radiation was periodically transmitted in three directions – vertical and tilted at angles of 76° to the horizontal direction in two mutually orthogonal planes. The vertical profiles of three wind velocity components $V_{mij}(z_k)$, where $m = x, y, z$ and i is the current number of measurement in the series $(i = 1, \ldots, N)$, were measured in 43 strobes z_j of the received signals of vertical extension $\Delta z = 5$ m at altitudes of 5–200 m. Series of $N = 150$ profiles were processed thereby providing 10- minute averaging of the results obtained. The components $\overline{E}_{\mathrm{MKE}}$ and $\overline{E}_{\mathrm{TKE}}$ were calculated as follows [9, 10]:

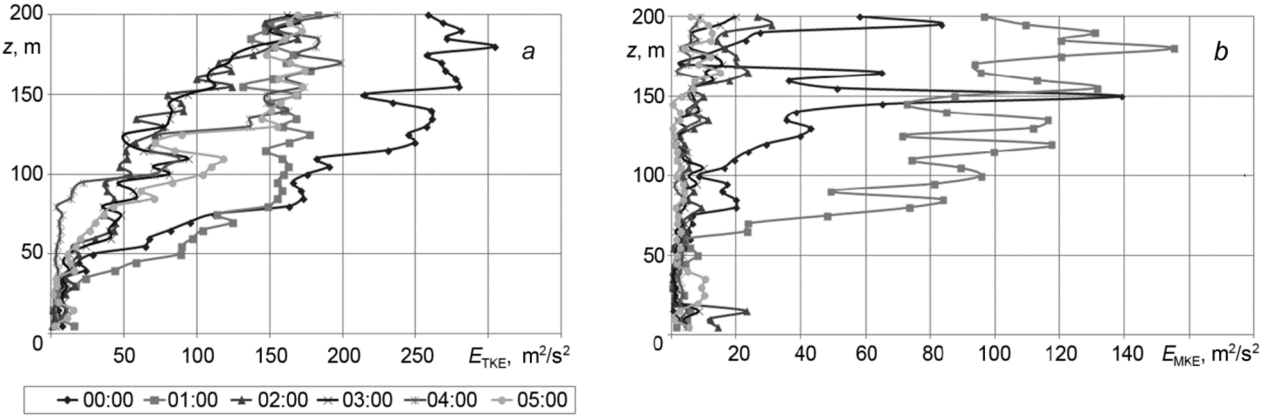

Fig. 1. Hourly dynamics of the wind kinetic energy components on September 12, 2006 at night from 00:00, local time, with 10-minute averaging. Here E_{TKE} is the turbulent kinetic energy (*a*), and E_{MKE} is the mean kinetic energy (*b*).

$$\bar{E}_{\mathrm{MKE}}(z_j,t_k)=\left[\left\langle V_x(z_j,t_k)\right\rangle^2+\left\langle V_y(z_j,t_k)\right\rangle^2+\left\langle V_z(z_j,t_k)\right\rangle^2\right]\Big/2$$

$$=\frac{1}{N^2}\left[\left(\sum_{i=1}^{N}V_{xij}\left(z_j,t_k\right)\right)^2+\left(\sum_{i=1}^{N}V_{yij}\left(z_j,t_k\right)\right)^2+\left(\sum_{i=1}^{N}V_{zij}\left(z_j,t_k\right)\right)^2\right]\Big/2, \tag{2}$$

$$\bar{E}_{\mathrm{TKE}}(z_j,t_k)=\left(\left\langle\sigma_x^2(z_j,t_k)\right\rangle+\left\langle\sigma_y^2(z_j,t_k)\right\rangle+\left\langle\sigma_z^2(z_j,t_k)\right\rangle\right)\Big/2=\frac{1}{N^2}$$

$$\times\left[\left(\sum_{i=1}^{N}V_{xij}\left(z_j,t_k\right)-\left\langle V_x\left(z_j,t_k\right)\right\rangle\right)^2+\sum_{i=1}^{N}\left(\left(V_{yij}(t_k)\right)-\left\langle V_y\left(z_j,t_k\right)\right\rangle\right)^2+\sum_{i=1}^{N}\left(\left(V_{zij}(t_k)\right)-\left\langle V_z\left(z_j,t_k\right)\right\rangle\right)^2\right]\Big/2, \tag{3}$$

where $\sigma_x^2(z_j, t_k)$, $\sigma_y^2(z_j, t_k)$, and $\sigma_z^2(z_j, t_k)$ are the variances of the *x*-, *y* - and *z*-components of the wind velocity in the *j*th strobe z_j of the *k*th measurement series started at time t_k, and <> denotes the averaging operator.

RESULTS AND DISCUSSION

Measurements were performed in the vicinity of Santa Clarita, California, USA [11] over a flat underlying surface without high vegetation during 7 days from 12 to 17 September, 2006. The weather was dry, warm, and sunny. Figures 1–3 show the vertical profiles of the kinetic energy components obtained by postprocessing of minisodar data. Times of the beginning of each 10-minute series of measurements are indicated in the figures. Figure 1 shows the dynamics of the kinetic energy components at night, Fig. 2 shows the diurnal hourly dynamics of the kinetic energy components, and Fig. 3 shows the hourly dynamics in the morning before noon.

In Fig. 1, attention is drawn to low values and small scatter of the turbulent kinetic energy component E_{TKE} in the lower 30-meter layer of the atmosphere. The maximum E_{TKE} values were observed at midnight. At 02:00, E_{TKE} increased with altitude in the lower 75-meter layer and decreased at higher altitudes. At z = 200 m, it decreased from 260 to 180 m^2/s^2, that is, by 31%. This tendency of the E_{TKE} decrease was observed till 03:00. Then E_{TKE} continued to

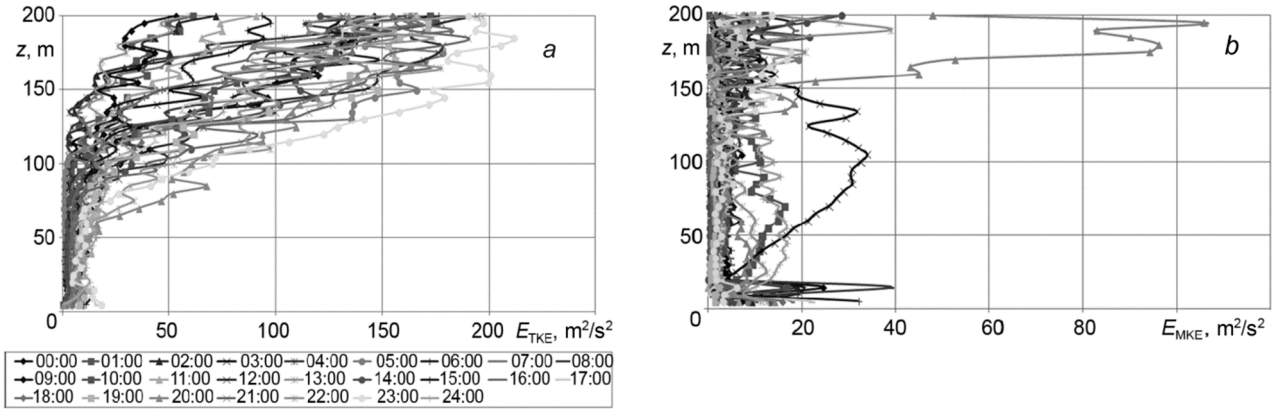

Fig. 2. Diurnal hourly dynamics of the wind kinetic energy components with 10-minute averaging from 00:00 on September 14, 2006. Here E_{TKE} is the turbulent kinetic energy component (*a*), and E_{MKE} is the mean kinetic energy component (*b*).

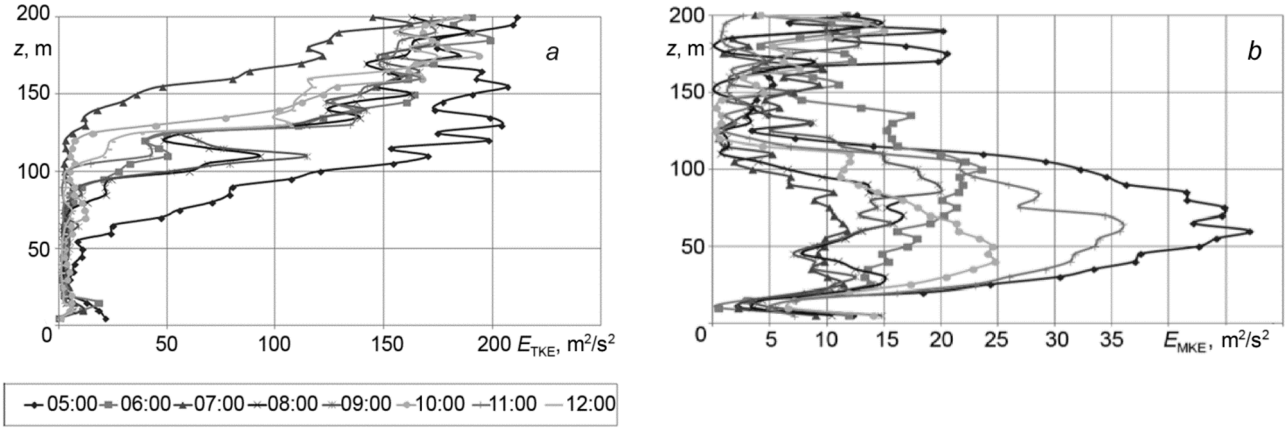

Fig. 3. Hourly dynamics of the wind kinetic energy with 10-minute averaging from 05:00 till 12:00 on September 15, 2006. Here E_{TKE} is the turbulent kinetic energy (*a*), and E_{MKE} is the mean kinetic energy (*b*).

decrease till 04:00 in the lower 100-meter layer, but increased at higher altitudes. By 05:00, E_{TKE} increased in the entire altitude range. The maximum E_{MKE} values on September 12, 2006 were recorded at 01:00, local time. Moreover, as can be seen from Fig. 1, the contribution of the mean kinetic energy component was about 2 times less than the contribution of the turbulent kinetic energy, and its altitude behavior was similar to that of E_{TKE}.

Analogous relationship between the contributions of E_{TKE} and E_{MKE} was observed for their diurnal behavior on September 14 shown in Fig. 2. The small spread of E_{TKE} values was observed to altitudes $z \approx 50$ m, and the largest one from $E_{TKE\,min} = 50$ m^2/s^2 at 09:00 to $E_{TKE\,max} = 200$ m^2/s^2 at 23:00 was observed at $z \approx 200$ m. From 10:00 till 12:00, the contribution of the mean kinetic energy in the lower 100-meter layer exceeded the contribution of the turbulent kinetic energy component, which is caused by the presence of the wind shear in the corresponding wind velocity profiles. From Fig. 2 it can also be seen that the vertical E_{MKE} profile increased in the morning from 05:00, reaches its maximum at 12:00, and then decreased toward midnight. The similar behavior of the kinetic energy components was noted in [3] for measurements with a FAS64 sodar in three altitude ranges z = 20–50, 50–80, and 80–110 m. According to [3], the diurnal behavior of the kinetic energy was also characterized by the presence of minima and maxima. It is obvious that

the time of their occurrence and their values depend on the meteorological conditions and the presence and characteristics of cloudiness and solar radiation.

Figure 3 illustrates the dynamics of the wind kinetic energy in the morning on September 15 2006 from 05:00 till 12:00 when the contribution of the mean wind kinetic energy to the total kinetic energy exceeded the contribution of the turbulent component in the lower 50-meter layer of the atmosphere. Thus, the character of the altitude dependence of E_{TKE} remained unchanged: low values and their small spread in near-surface layer up to z = 50 m and its subsequent increase at higher altitudes. The maximal value of the turbulent kinetic energy was observed at z = 200 m at 05:00, and its minimal value was observed at 07:00, local time.

During measurements on September 12, 14, and 15, 2006, the total turbulent kinetic energy changed from several tens to several hundreds m^2/s^2, which is in agreement with the available literature data [3, 12]. From Figs. 1–3 it can be seen that the turbulent kinetic energy increases with sounding altitude z, and in the near-surface layer up to 25–50 m, it weakly depends on z. Thus, it changed from 10 to 90 m^2/s^2 at z = 25 m on September 12, and on September 14 and 15, it weakly changed with altitude up to z = 50 m. The spread in values of the total kinetic energy also increased with z, and at an altitude of 200 m, it changed already from 70 to 200 m^2/s^2, that is, almost tripled during the day. The similar behavior of the kinetic energy was noted in [3, 12].

Thus, based on the data presented above we can conclude that the kinetic energy value in the surface layer at attitudes of 25–100 m depends weakly on the sounding altitude z and increases with further increase in z. The diurnal behavior of radiative heating of the earth surface causes the presence of minima and maxima of the kinetic energy, and the time of their occurrence depends on the meteorological conditions of observations.

Let us consider the altitude dependence of the horizontal wind velocity averaged over 10-minite periods and the spatiotemporal dynamics of the wind velocity vector. Figure 4 shows the altitude dependences of the horizontal wind velocity V_{av} and its component V_x and V_y (measurements from 11:00 till 23:00 on September 13, 2006). It can be seen that at altitudes from 5 to 100 m, the horizontal wind velocity and its components V_x and V_y are relatively stable. Significant changes in the horizontal velocity and its component were observed at altitudes from 100 to 200 m practically at any time.

This situation is due to the fact that in the surface layer, the mean wind velocity and its turbulent fluctuations are significantly slowed down because of the interaction of air masses with the motionless underlying surface. As the altitude increases from 100 to 200 m, considerable turbulent fluctuations of the wind velocity and its component are observed, that is, the effect of the turbulence is intensified. The maximum effect of the turbulence is observed at altitudes of 150–200 m, and this altitude range poses the greatest threat to UAV.

The time of day also influenced significantly on the results of observations. In the afternoon, as can be seen from Fig. 4, no significant fluctuations of the horizontal wind velocity were observed at all altitudes. The V_x and V_y components also underwent no significant fluctuations. The situation started to change during a sunset (at about 17:00). At altitudes of 100–200 m, significant fluctuations of the horizontal wind velocity with altitude were observed. They lasted till 19:00. We believe that this situation was caused by the termination of the light day and the beginning of inhomogeneous cooling of the Earths surface. Thus, from 16:00 till 19:00, the wind velocity values sharply changed from layer to layer. Moreover, from 16:00 and to the end of the observation period (23:00), the horizontal velocity components V_x and V_y differed considerably.

Figure 5 shows the diurnal hourly dynamics of the wind velocity vector (northern direction is upwards, southern is downwards, eastern is to the right, and western is to the left) from 05:00 on September 16 to September 17. The velocity scale is shown in the figure. From the figure it can be seen that at any time, the direction of the horizontal wind velocity does not undergo sharp changes from layer to layer up to ~100 m. The wind direction changes in the layer from 100 to 200 m and whereas from 05:00 (sunrise at 05:00) to 06:00 these changes begin from an altitude of 150 m and higher, from 07:00 to 08:00 they begin already from an altitude of 100 m. This can be attributed to inhomogeneous heating of the Earth surface cooled at night. From 09:00 till 10:00, the lower boundary of the turbulent layer rises again to 150 m, and by 14:00, it reaches 200 m. A repeated decrease in the lower turbulent layer boundary can be seen from 16:00 till 18:00. In the daytime (from 05:00 till 17:00), the value of the wind velocity considerably exceeds the corresponding night values (from 18:00 on September 16 to 03:00 on September 17, 2006). In the daytime, the maximal values of the wind velocity were recorded in the morning (from 04:00 till 06:00–07:00) and daytime (from 09:00 till 16:00–17:00). The minimal values of the wind velocities were observed at night (from 22:00 till 03:00).

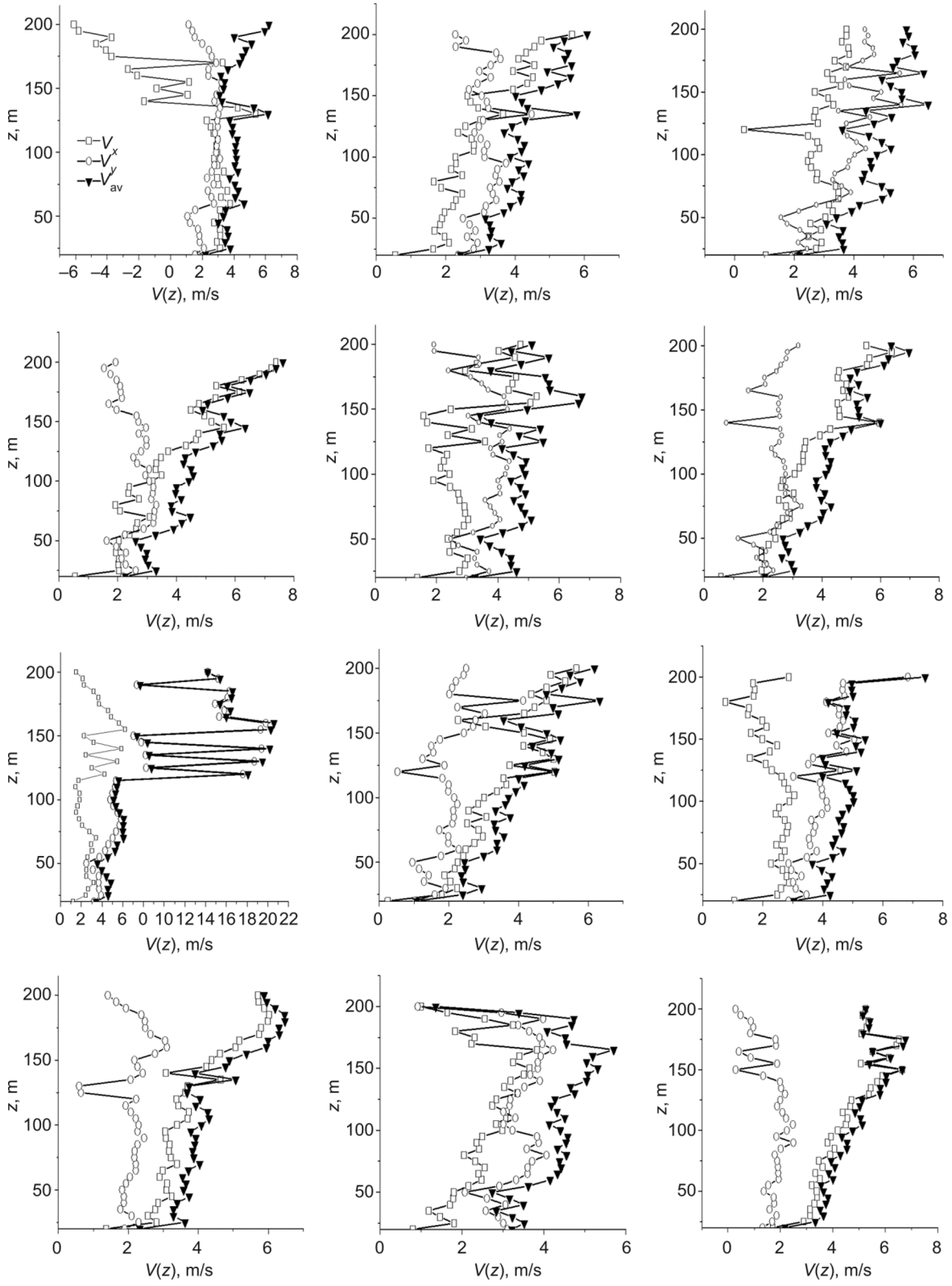

Fig. 4. Diurnal hourly behavior of the mean horizontal velocity V_{av} and its components V_x and V_y averaged over 10-minute periods and retrieved from minisodar measurements from 11:00 till 23:00 on September 13, 2006.

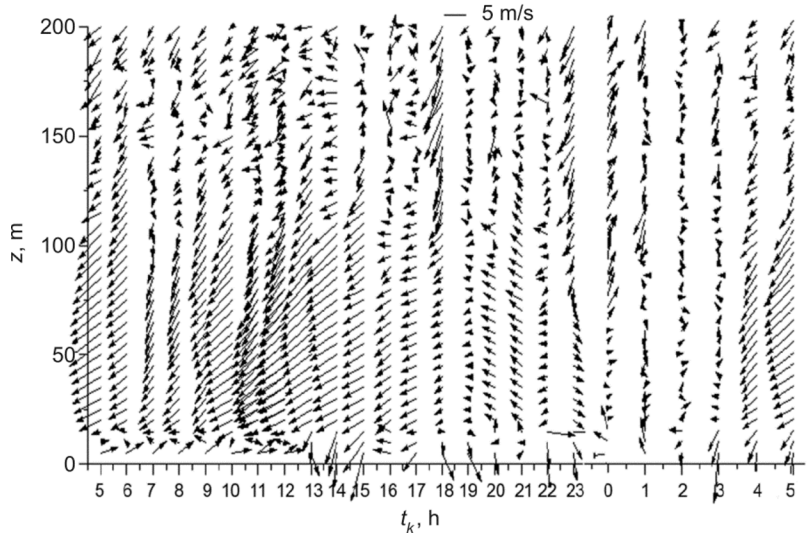

Fig. 5. Spatiotemporal dynamics of the wind velocity vector from 05:00 on September 16 till 05:00 on September 17. The scale of the wind velocity is shown in the figure. Here northern direction is upward, southern is downward, eastern is to the right, and western is to the left.

The following should be specially noted. Based on visual analysis of Figs. 4 and 5, we can conclude that during periods of enhanced perturbations (active influence of the turbulence), the linear sizes of the perturbation regions are commensurable with the spatial resolution Δz = 5 m of the employed observation method. This can be seen, for example, from 07:00 till 11:00 on September 16 and from 01:00 till 03:00 on September 17 (Fig. 5). These perturbations pose the greatest danger to small-size UAV.

Thus, the reduced kinetic energy of the atmosphere and its components have been estimated in the lower 200-meter layer of the atmosphere by postprocessing of minisodar measurements of the spatiotemporal dynamics of three wind velocity components and their variances focusing on the turbulent kinetic energy component. The turbulent kinetic energy in the near-surface layer was very low up to ~50 m during a 24 hour period of continuous observations. This is due to the fact that the wind velocity and the turbulent motion are significantly slowed down due to the interaction of air masses with the motionless earth surface. The turbulent kinetic energy quickly increased in the altitude range from 50 to 100 m, and at altitudes above 100 m, its strong increase was observed. The turbulent kinetic energy reached its maximum at altitudes of 150–200 m. This layer poses the greatest danger to UAV flights.

CONCLUSIONS

The kinetic energy values have been estimated by postprocessing of minisodar measurements of the spatiotemporal dynamics of three wind velocity components and their variances in the lower 200-meter layer of the atmosphere. The analysis of the vertical profiles of the kinetic energy in the atmospheric boundary layer showed that up to ~50 m, the turbulent kinetic energy E_{TKE} is low, its spread is small, and it sharply increases at higher altitudes.

The maximal E_{TKE} values were observed at midnight together with the maximal E_{MKE} values. In the morning, the contribution of the mean kinetic energy in the lower 100-meter layer of the atmosphere exceeded the contribution of the turbulent kinetic energy. This can be explained by the presence of wind shears in the corresponding profiles of the wind velocity vector. The E_{MKE} values increased in the morning, reached their maximal values by noon, and then decreased toward midnight. During measurements, the total kinetic energy of unit air mass changed from several tens to several hundreds m^2/s^2 (J/kg). The diurnal behavior of the kinetic energy was characterized by the presence of several

maxima and minima the time of occurrence and the values of which depended on the meteorological conditions of observations and the presence and the characteristics of cloudiness and solar radiation.

Based on the foregoing, we can conclude that during periods of maximal perturbations (active turbulent motions of air masses), the linear sizes of perturbation regions were commensurable with the spatial resolution $\Delta z = 5$ m of the employed observation method. The possibility of revealing times of the maximal and minimal turbulence, that is, of the most and least favorable times for UAV flights was illustrated.

This work was performed within the framework of the State Assignment to the V. E. Zuev Institute of Atmospheric Optics of the Siberian Branch of the Russian Academy of Sciences.

REFERENCES

1. G. Schlichting, The Theory of the Boundary Layer [Russian translation], Nauka, Moscow (1974).
2. T. Foken, Micrometeorology, Springer Verlag, Berlin; Heidelberg (2008).
3. M. A. Haggagy, A Sodar-Based Investigation of the Atmospheric Boundary Layer, Berichte des Meteorologischen Institutes des Universität Freiburg, No. 8, Freiburg (2003).
4. M. Yu. Kuprikov, Unmanned Aerial Vehicle, Great Russian Encyclopaedia [Electronic resource], https://bigenc.ru/technology_and_technique/text/4087725 (Reference Date: October 1, 2020).
5. V. A. Banakh and I. N. Smalikho, Coherent Doppler Wind Lidar in a Turbulent Atmosphere [in Russian], Publishing House of the Institute of Atmospheric Optics of the Siberian Branch of the Russian Academy of Sciences, Tomsk (2013).
6. V. V. Sterlyadkin, A. G. Gorelik, and G. G. Shchukin, in: Abstracts of Lectures. Ser. "III All-Russian Armand Readings: Youth School," (2013), pp. 24–42.
7. S. Bradley, Atmospheric Acoustic Remote Sensing, CRC Press, Boca Raton (2008).
8. R. L. Coulter and M. A. Kallistratova, Meteor. Atmos. Phys., **85**, Nos. 1–3, 3–19 (2004).
9. L. G. Shamanaeva, A. I. Potekaev, N. P. Krasnenko, and O. F. Kapegesheva, Russ. Phys. J., **61**, No. 12, 2282–2287 (2018).
10. M. V. Tarasenkov, N. P. Krasnenko, and L. G. Shamanaeva, Program for Constructing the Altitude-Temporal Distribution of Wind Velocity Components in the Lower Atmosphere from the Data of Acoustic Sounding, RF Certificate of State Registration of Computer Program No. 2016619428, Rospatent, Moscow (2016).
11. K. H. Underwood and L. G. Shamanaeva, Russ. Phys. J, **53**, No. 11, 526–532 (2011).
12. G. B. Greenhut and G. Mastrantonio, J. Appl. Meteor., **28**, 99–106 (1989).